PHYSICAL REVIEW B VOLUME 12, NUMBER 5 1 SEPTEMBER 1975

EPR line broadening and magnetic phase transitions in antiferromagnetic FeP_3O_9

Alvin Kiel*
Instituto de Física, Universidade Estadual de Campinas, Campinas, S.P., Brazil
(Received 28 May 1974)

The EPR linewidths of polycrystalline samples of antiferromagnetic ferric metaphosphate (FeP_3O_9) has been measured in the range $0.01 \leq T - T_N < 100$ K ($T_N = 9.3$ K). The widths were fitted to a power-law form $(T - T_N)^\gamma$. In the reduced-temperature range $0.03 < \epsilon < 0.7$ [$\epsilon \equiv (T - T_N)/T_N$], the best fit gives $\gamma \cong -0.67$. For $\epsilon < 0.02$, the change in linewidth is very slight. At high temperatures such that $\epsilon > 1$, far above the critical regime, we obtained $\gamma \cong -1.65$. These results are quite similar to some recent results of Birgeneau on $NiCl_2$. Spin-flip transitions have been observed from individual crystallites in the polycrystalline samples at 4.2 and 1.6 K. By cycling the magnetic field and temperature we obtain a signal at 4.2 K which exactly mimics the EPR signals for $T > T_N$ ($T_N = 9.3$ K) with no sign of the spin-flop transitions. This implies a striking hysteresis in the H-T phase diagram.

I. INTRODUCTION

Ferric metaphosphate (FeP_3O_9) is a nearly colorless, crystalline material first prepared by Brasseur.[1] The crystal is monoclinic[1] and generally the growth habit leads to small, needlelike single crystals (1×0.05 mm^3). Since ferric compounds are rarely clear in the visible, it attracted some interest in the early 1960s as a potential Faraday rotation modulator.[2] However, in the glassy state, it was found that the optical loss is very large throughout the visible spectrum. Evidently the PO_3 complex is strongly bound in the crystalline phase so that the Fe^{3+} – O charge-transfer bands are well into the ultraviolet (~3250 Å, see Ref. 1). In the glassy state, the coordination changes sufficiently for the charge-transfer band to move into the visible region, typical of ferric oxides. Berger *et al.*[2] have investigated the magnetic properties of FeP_3O_9 and report an antiferromagnetic transition at 10.6 K. This measurement was repeated in the course of this study (by R. C. Sherwood of Bell Labs.) and we find the Néel point is 9.5 ± 0.4 K (see Fig. 1). The linewidth studies, discussed in Sec. II, narrow this range to $T_N = 9.3 \pm 0.05$ K. The Curie-Weiss temperature extrapolates to 10.9 ± 2 K (this involves using some higher-temperature data not shown in Fig. 2), in reasonable agreement with Ref. 2. The variation in magnetization with magnetic field at 1.55 K is shown in Fig. 2. There is some indication that the magnetization remains nonzero at zero applied field, implying a slight canting of the sublattices (or canted ferromagnetism). The sensitivity of the apparatus is, however, not sufficient to be certain of the canting, since the indicated residual magnetization $4\pi M$ is only 23 Oe, barely outside experimental error.

The effective magneton number calculated from the susceptibility data was determined to be 5.9, clearly indicating Fe^{3+} with the "high spin," $^6S_{5/2}$ ground state. (The theoretical magneton number is 5.92.) The paramagnetic-resonance signal at X band (~9 GHz) was obtained for a coarse-powder sample. At room temperature, a single structureless line is observed with $g = 2.025 \pm 0.025$ with a half-width of 325 G. The large linewidth made a more accurate determination of the g value very difficult. Using several small crystals with approximately the same alignment relative to the cavity did not lead to structure in the signal or change in linewidth. To the accuracy of this measurement, the EPR signal is isotropic.

II. LINE BROADENING ABOVE T_N

The Néel temperature of FeP_3O_9 is rather low for ferric compounds. It is still in a region, however, where variable-temperature measurements are easy using variable-temperature Dewars. It appeared, therefore, to be a good material to observe critical broadening of the paramagnetic-resonance signal at especially low temperatures.

A conventional X-band EPR apparatus was employed using a direct video-detection system. To minimize coupling of absorption and dispersion signals, low-Q (~1000) under-coupled cavities were used. A Janis Varitemp Dewar could vary the temperature between 5 and 100 K. The helium-flow rates were kept as high as feasible and microwave power as low as possible to minimize sample heating. A carefully calibrated carbon resistor (47 Ω, $\frac{1}{4}$ W) was used to determine cavity temperature. In Fig. 3 we show a series of X-Y recorder tracings of the EPR absorption signal as a function of $T - T_N$. The Néel temperature was chosen as the point where the EPR signal seemed to disappear. From the average of 10 runs, a value of $T_N = 9.3 \pm 0.05$ was taken as the Neel temperature. However, in each series such as that depicted in

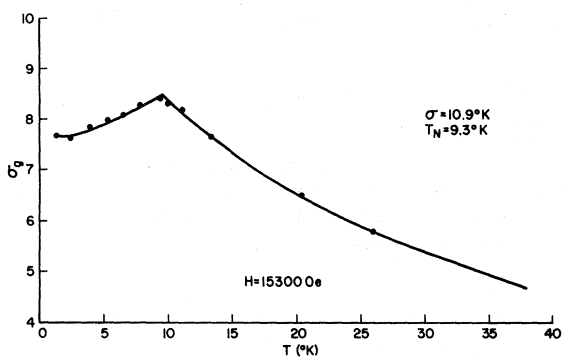

FIG. 1. σ_g (magnetization/g) of FeP_3O_9 as a function of temperature.

Fig. 3, $T - T_N$ represents a measurement of temperature relative to the plot chosen to represent T_N. The reproducibility of T_N was < 50 mK.

The broadening of the EPR line as T approaches T_N is clearly visible in the set of curves displayed in Fig. 3. There is also a shift of the absorption peak to lower field as we approach T_N. Similar behavior has been observed[3] in Cr_2O_3 and in several manganese monocalcogenides.[4] More recently, Seehra[5] has investigated EPR linewidths in MnF_2 near the critical point ($T_N = 67$ K), and Birgeneau *et al.*[6] have studied $NiCl_2$ ($T_N = 49.5$ K). Our measurements are at a much lower temperature than any of the previous works.

The data from many runs are plotted as a function of $T - T_N$ in Fig. 4. The exponent of $T - T_N$, $|\gamma|$ is far less than 1.6 in the nieghborhood of the Néel point. Note that far above the critical region $9 \leq T - T_N \leq 100$ K, $1 < \epsilon < 10$, where ϵ is reduced temperature [$\epsilon \equiv (T - T_N)/T_N$], γ is reasonably close

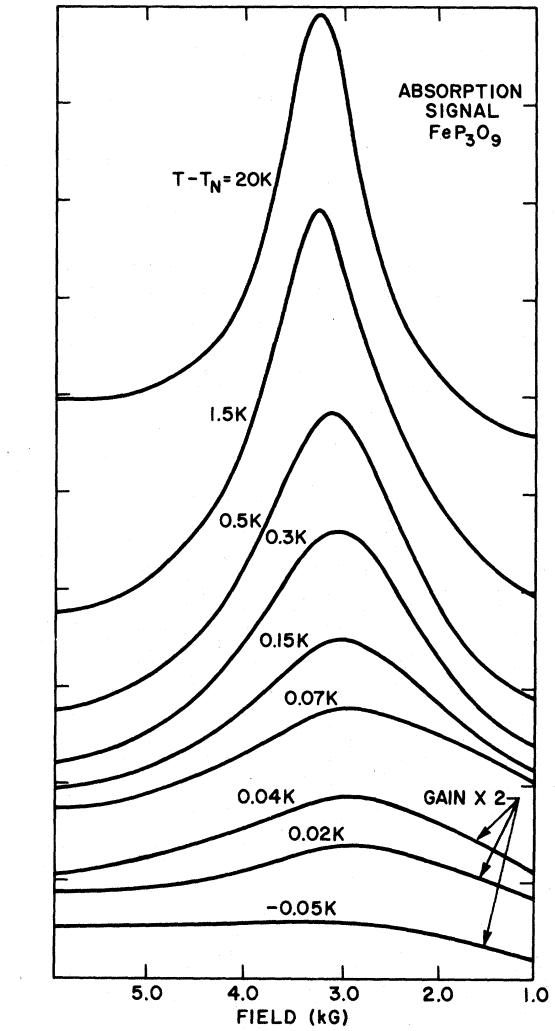

FIG. 3. EPR absorption vs H for various $T - T_N$ ($T_N = 9.3$ K).

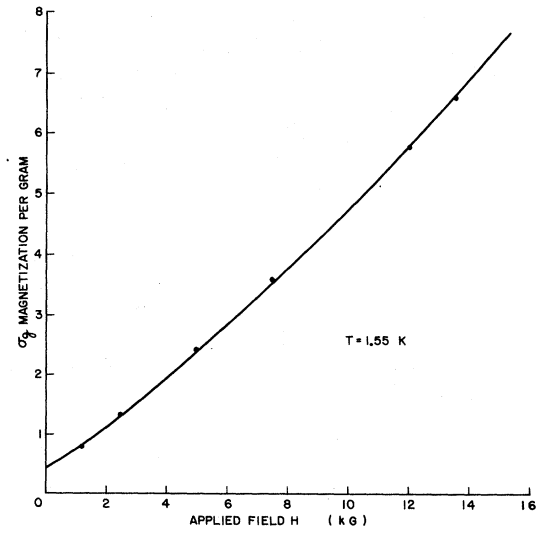

FIG. 2. σ_g (magnetization/g) of FeP_3O_9 as a function of field ($T < T_N$).

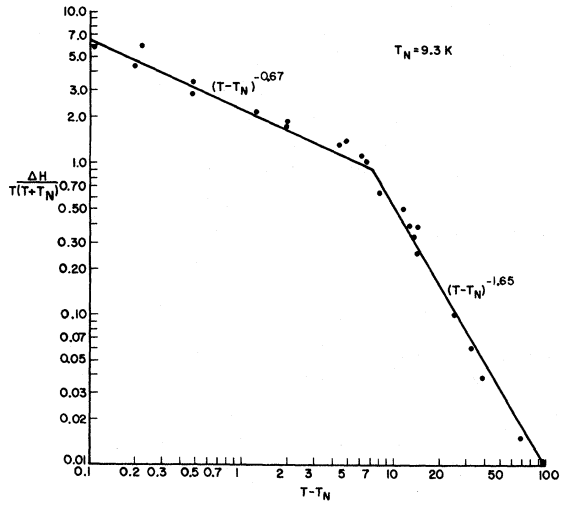

FIG. 4. $\Delta H(\chi_T/T)$ vs $T - T_N$ (arbitrary units).

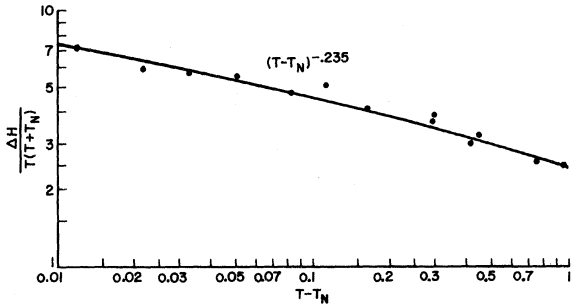

FIG. 5. $\Delta H(\chi_T/T)$ vs $T-T_N$ (very small $T-T_N$). The ordinate has same units as Fig. 4. For ΔH, only the width on the high-field side of the line was used.

to -1.6. Below $T-T_N = 9$ K, $0.2 < \epsilon < 1$, a rather crude fit gives $\gamma \sim 0.68$. (Note that the break point for the two curves is chosen quite arbitrarily.)

At very low $T-T_N$, the linewidth measurements are difficult due to asymmetry of the absorption line and loss of sensitivity. Using only the half-width on the high-field side of the absorption line, we obtain the data shown in Fig. 5 for $0.01 < T-T_N \leq 1.0$ K, $0.001 < \epsilon < 0.1$. A rough fit to $(T-T_N)^\gamma$ gives $\gamma = -0.235 \pm 0.03$ in this region.

The product of integrated signal strength S and temperature T is plotted against $T-T_N$ in Fig. 6. It can be seen that even for temperatures far above T_N, there is a definite reduction in the product ST.

III. DISCUSSION

A current theory of critical broadening above T_N is based on the relaxation of spin fluctuations in the random-phase approximation (RPA). The theory of the critical broadening is described in Ref. 7(a). Basically, this theory shows that the temperature-dependent part of the linewidth is proportional to a function $A(T)$. The function $A(T)$ may be evaluated using the RPA in the limit of *isotropic fluctuations* and some simplifications in the q-space summations. The result is

$$A(T) \sim (T/\chi_T)\xi^{5/2}, \tag{1}$$

where ξ is a correlation length for the spin fluctuations. The correlation length must be a function of $T-T_N$. Neutron-diffraction experiments[10] give

$$\xi \sim (T-T_N)^{-0.63}, \qquad A(T) \sim (T/\chi_T)(T-T_N)^{-1.575}. \tag{2}$$

The data in the high-temperature region of Fig. 4 can be fitted to $(T-T_N)^\gamma$, where $\gamma = -1.65 \pm 0.2$, which conforms quite well with Eq. (2) but at temperatures well outside the critical regime. This result is undoubtedly fortuitous. In the range $0.1 < T-T_N < 10$ K, we obtain $\gamma \simeq -0.675 \pm 0.1$. This result is essentially the same as that observed by Birgeneau *et al.*[6] They point out that if Eq. (1) is replaced by

$$A(T) \sim (T/\chi_T)\xi \tag{3}$$

instead of the RPA result $\xi^{5/2}$, good agreement is obtained. The agreement between our results and Ref. 6 is rather surprising since the crystal systems and Néel temperatures are so different.

The results for very small $T-T_N$, Fig. 5, are included primarily for completeness. As stated previously, the EPR lines in this regime are very asymmetric with some signal even at $H=0$. We do not claim any special significance to taking the half-width on the high-field side of the line. However, the results are consistent with $A(T)$, displaying a more "gentle" temperature dependence for at least one of the crystal axes when $T-T_N < 0.3$ K ($\epsilon < 0.03$). Other factors which may contribute to this behavior are (i) the difficulty of placing T_N exactly and (ii) a slight variation of T_N with crystal axis. The power-law fit in Fig. 5 is for purposes of comparison only. Perhaps a better description of this data is to claim that the broadening saturates when $\epsilon < 0.03$.

Figure 6 may at first appear surprising; a normal paramagnetic substance would not be expected to show a decrease in the product ST at low temperatures. However, it is well known that short-range order may be manifested well above the critical temperature. The formation of "exchange pairs" will occur at the expense of the main resonance intensity.

IV. ANTIFERROMAGNETIC RESONANCE AND MAGNETIC PHASE TRANSITIONS

At 12 GHz, no magnetic resonance signal for $H < 25\,000$ G was observed at any temperature below T_N. This also proved to be the case at 18 GHz for $H < 25\,000$ G. The resonance signal in a 34 GHz spectrometer (derivative) at 4.2 K is shown in Fig. 7. The structure is due to unresolved spin-flop transitions[11-14] in the polycrystalline sample. At 1.6 K, spin-flop transitions from individual crystallites are clearly evident (see Fig. 8). Note that

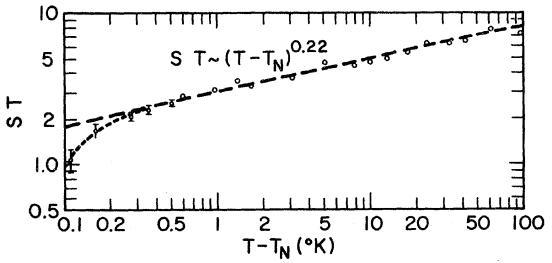

FIG. 6. Product of line strength (S) and temperature vs $T-T_N$.

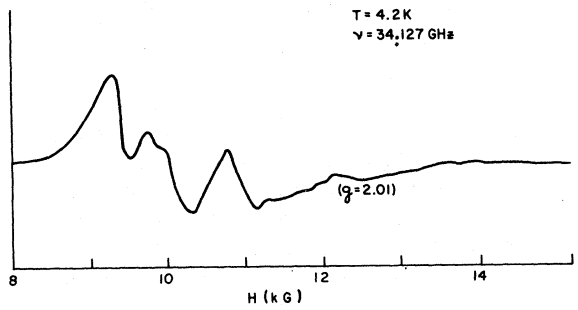

FIG. 7. Magnetic-resonance signal ($d\chi''/dH$) at 4.2 K, $\nu = 34.127$ GHz.

the low-field edge of the resonance signal has moved approximately 1000 G toward higher fields at 1.6 K as compared to 4.2 K. The signal also extends to much higher magnetic fields at 1.6 K, and indeed, there still seems to be small signal present at 14 kG. From the 1.6-K data, we obtain a critical field[15-17]

$$H_c = [2\lambda K_{\min}/(1-\alpha)]^{1/2} \simeq 9.6 \text{ kG}, \tag{4a}$$

if

$$\alpha = \frac{\chi_{\parallel}}{\chi_{\perp}} \simeq 0 . \tag{4b}$$

The large amount of structure seen in Fig. 8 indicates that spin-flop resonance signals may be seen from crystallites which have a large angular misalignment. This is more common in low-symmetry crystals (as in the present case) than in uniaxial crystals such as MnF_2.

If the direction of the magnetic sweep is reversed (H is increasing in Fig. 8), the features seen in Fig. 8 are shifted ~ 230 G towards lower fields. This small hysteresis, representing a change in the critical fields of only about 4.6%, is typical of the first-order spin-flop transition. In the case of uniaxial crystals, the hysteresis can be represented

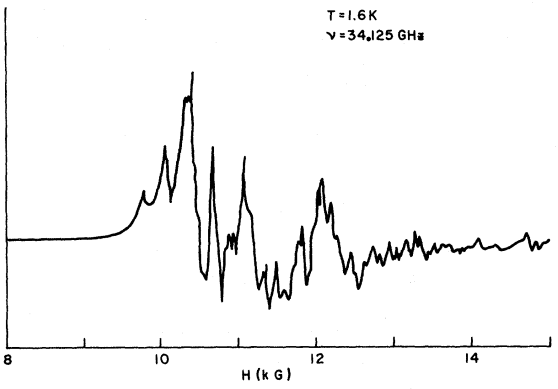

FIG. 8. Magnetic-resonance signal ($d\chi''/dH$) at 1.6 K, $\nu = 34.125$ GHz.

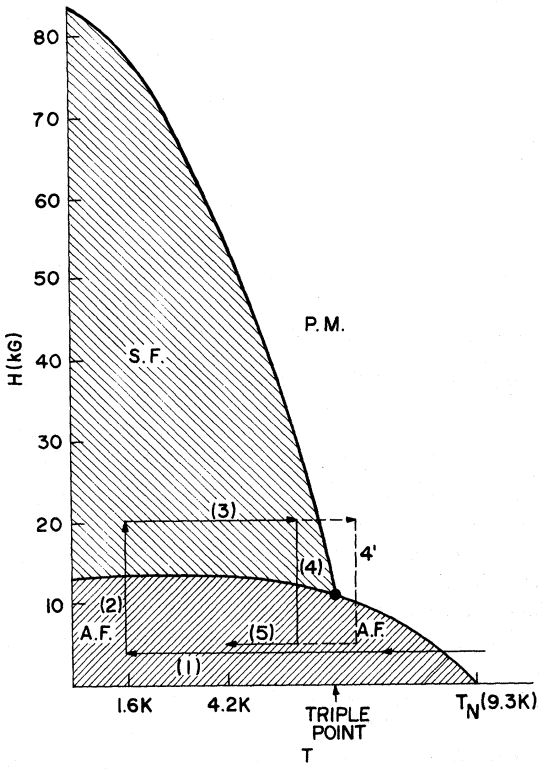

FIG. 9. Phase diagram near AF-SF-PM triple point. The diagram is just an approximation based on Ref. 23. Since the triple point is hardly more than a guess, the two possible paths are shown.

by

$$\frac{H_c(\text{AF}\rightarrow\text{SF})}{H_c(\text{SF}\rightarrow\text{AF})} = \frac{2H_E + H_A}{2H_E - H_A} , \tag{5}$$

where AF and SF represent antiferromagnetic phase and spin-flop phase, respectively, and H_E, H_A are exchange and anisotropy fields. For the observed hysteresis, Eq. (5) predicts $H_A/H_E \simeq 0.023$ and $H_E = 44.8$ kG.

The AF $\rightleftarrows$ SF transition is just one of a class of magnetic-field-induced transitions. A second well-known transition SF $\rightleftarrows$ PM (spin-flop to paramagnetic) can occur at still higher fields. Although AF $\rightleftarrows$ SF has been observed in many materials by a variety of techniques[11,14,18,19] (including magnetic resonance), the SF $\rightleftarrows$ PM has rarely been observed[18,20] and never in EPR. There is considerable literature on the theory of this transition in uniaxial materials.[21-23] Yamoshita[24] has described the stability conditions for AF, SF, and PM phases (as well as two new magnetic phases which will not concern us). A phase diagram is illustrated in Fig. 9.

As discussed above, the AF $\rightleftarrows$ SF transition is a first-order transition with a discontinuity in the magnetization. The SF to PM is a second-order

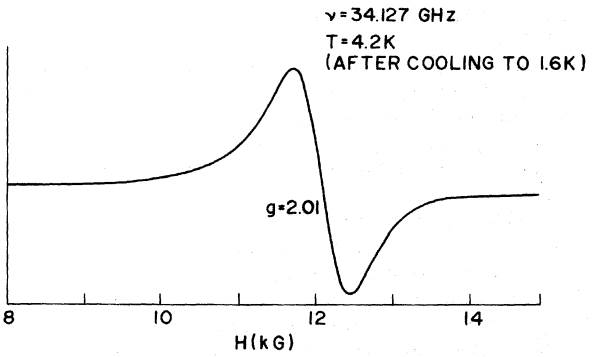

FIG. 10. Magnetic-resonance signal ($d\chi''/dH$) at 4.2 K, $\nu = 34.125$ GHz. This signal was obtained by increasing H to 15 kG at 1.6 K, increasing temperature to between 4.2 and ~7 K, allowing temperature to settle at 4.2 K, and finally reducing field to 5 K.

phase transition with continuous change in the magnetization. The critical field for SF → PM, H_c (SF → PM) is, according to spin-wave theory, given by

$$H_c(\mathrm{SF} \rightarrow \mathrm{PM}) = 2H_E - H_A \simeq 2H_E \,. \qquad (6)$$

This field [~89 kG according to Eq. (5)] is far out of our reach at 1.6 K. However, by warming the sample up in a 15 kG field, the SF → PM transition can be reached at a temperature well below T_N. In this case, the temperature was about 5–7 K. (The cavity was lifted out of the helium for a few seconds.) The sample was then allowed to reach 4.2 K, and the field reduced to 5 kG. The temperature-field path is illustrated in Fig. 9. The resonance spectrum obtained is shown in Fig. 10, which should be compared with Fig. 7. The signal appears to be the paramagnetic-resonance signal and was observed for periods of from 3 to 15 min (the maximum attempted) after the cycle. The linewidth observed was about the same as that seen at 14 K in the critical linewidth studies.

It is important to note that we do not know the triple-point temperature and can not be certain we entered the PM regime. This is why we show two possible paths in Fig. 9. It has been pointed out to me that if the anisotropy is small, the frequency of one of the normal modes in the SF state may be close to γH so long as H is not too close to the critical field. Thus the resonance signal in Fig. 10 may not be unique to the PM phase although it is *certain that it does not correspond to the AF regime*. It should be noted that the total signal strength in Fig. 10 corresponds closely to the strength observed in the PM regime for $T > T_N$. If the sample is cooled to 1.6 K, the SF signal in Fig. 5 returns and the system can be recycled to obtain the "PM" signal in Fig. 10. However, if the sample temperature is allowed to warm well above T_N, the 4.2-K spectrum becomes identical to Fig. 7; that is, we have passed into the AF phase in the temperature-field cycle.

The signal observed in Fig. 10 was unexpected.[25] The result implies a very large hysteresis in the phase boundaries on an H-T diagram. In fact, what seems to be required is for the triple point ($4.2 < T_t < \sim 7$ K, $H_t \sim 6$–9 kG) to move below 4.2 K and/or H_t to move to lower fields in the temperature-field cycle described.

In much of the previous work, we have relied on theories developed for uniaxial crystals and obviously are on "shaky" ground in applying these to the present case. Surprisingly, the critical-broadening results were very similar to experiments on more symmetric materials. In the case of the SF → PM phase transition, we may be stretching the analog to simpler systems too far. In any case, the observation of a simple EPR-like signal paramagnetic at 4.2 K and $5 \leq H \leq 15$ kG is a very striking result.

ACKNOWLEDGMENTS

I am indebted to R. C. Sherwood for taking the magnetic-susceptibility data and to W. M. Walsh for allowing the use of his EPR setup for the spin-flop and magnetic-transition result. L. W. Rupp's assistance in those experiments was very helpful. Heinz Weber supplied most of the crystals and worked out the composition. C. B. Rubinstein pointed out the earlier work in Ref. 1. Don Olson helped with X-band data.

*Former address: Bell Labs., Holmdel, N. J. Most of this work was performed at Bell Labs.

[1]P. Brasseur, Bull. Soc. Chim. Fr. 13, 261 (1946).
[2]S. B. Berger, C. B. Rubinstein, R. C. Sherwood, A. W. Treptow, and H. J. Williams (unpublished).
[3]T. R. McGuire, E. J. Scott, and F. H. Grannis, Phys. Rev. 102, 1000 (1956).
[4]L. R. Maxwell and T. R. McGuire, Rev. Mod. Phys. 25, 279 (1953).
[5]Molindar S. Seehra, J. Appl. Phys. 42, 1290 (1971); M. S. Seehra and T. G. Castner, Solid State Commun. 8, 787 (1970); Molindar S. Seehra, Phys. Rev. B 6, 318 (1972).
[6]R. J. Birgeneau, L. W. Rupp, H. J. Guggenheim, P. A. Lindgard, and D. L. Huber, Phys. Rev. Lett. (to be published).
[7](a) D. L. Huber, Phys. Rev. B 6, 3180 (1972); (b) J. Phys. Chem. Solids 32, 2145 (1971).
[8]Strictly speaking, this is true of uniaxial crystals. Iron metaphosphate is actually monoclinic.
[9]The factor T in ST is to account for the Boltzman statistical factor. As we approach T_N, one would not expect this form to be meaningful.
[10]A. Tucciarone, H. Y. Lau, L. M. Corliss, A. Delapa-

line, and J. M. Hastings, Phys. Rev. B 4, 3206 (1971). These experiments were on $RbMnF_3$.
[11]Meneyuki Date and Kazukiyo Nagata, J. Appl. Phys. 34, 1038 (1963).
[12]Meneyuki Date, J. Phys. Soc. Jpn. 16, 1337 (1961).
[13]T. Nagamiya, K. Yosida, and K. Kubo, Adv. Phys. 4, 2 (1955). J. Kanamori and M. Tochiki, J. Phys. Soc. Jpn. Suppl. 17, 64 (1962).
[14]M. Abkowitz and A. Honig, Phys. Rev. 136, A1003 (1964).
[15]C. J. Gorter, Rev. Mod. Phys. 25, 277 (1953).
[16]I. S. Jacobs, J. Appl. Phys. Suppl. 32, 61 (1961).
[17]K. Yosida, Prog. Theor. Phys. 7, 25 (1952); J. Ubbink, Physica 19, 9 (1953).
[18]I. S. Jacobs and P. E. Lawrence, Phys. Rev. 164, 866 (1967).
[19]Simon Foner, in *Magnetism*, edited by G. T. Rado and H. Suhl (Academic, New York, 1963), Vol. I, pp. 388–415 and references therein.
[20]H. Rives, Phys. Rev. 162, 491 (1967).
[21]H. Rohrer and H. Thomas, J. Appl. Phys. 40, 1025 (1969).
[22]J. Fedder and E. Pytte, Phys. Rev. 168, 640 (1968).
[23]Frederic Keffer, in *Encyclopedia of Physics*, edited by H. P. Wijn (Springer, Berlin, 1966), pp. 134–140.
[24]Naohiko Yamashito, J. Phys. Soc. Jpn. 32, 610 (1972).
[25]We know that H_c(AF → SF) is ~8.5 kG at 4.2 K. The EPR results imply that we never enter the AF region.